Review of Theoretical Studies for Prediction of Neurodegenerative Inhibitors

F. Prado-Prado*,[1] and I. García[2]

[1]*Department of Organic Chemistry, University of Santiago de Compostela, Spain*

[2]*Department of Organic Chemistry, University of Vigo, Spain*

Abstract: Alzheimer's disease (AD) is characterized by several pathologies, this disease is a neuropathological lesion in brain. Indeed, a wealth of evidence suggests that β-amyloid is central to the pathophysiology of AD and is likely to play an early role in this intractable neurodegenerative disorder. AD is the most prevalent form of dementia, and current indications show that twenty-nine million people live with AD worldwide, a figure expected rise exponentially over the coming decades. Clearly, blocking disease progression or, in the best-case scenario, preventing AD altogether would be of benefit in both social and economic terms. However, current AD therapies are merely palliative and only temporarily slow cognitive decline, and treatments that address the underlying pathologic mechanisms of AD are completely lacking. While familial AD (FAD) is caused by autosomal dominant mutations in either amyloid precursor protein (APP) or the presenilin (PS1, PS2) genes. First, we revised 2D QSAR, 3D QSAR, CoMFA, CoMSIA and Docking of *β* and *γ*-secretase inhibitors. Next, we review 2D QSAR, 3D QSAR, CoMFA, CoMSIA and docking for GSK-3*α* and GSK-3*β* with different compound to find out the structural requirements.

Keywords: QSAR, CoMSIA, COMFA, Docking, *β*-secretase inhibitors, *γ*-secretase inhibitors, Alzheimer's disease (AD).

INTRODUCTION

Pathologically, Alzheimer's disease (AD) is characterized by the accumulation of amyloid beta peptide (Aβ), as fibrillar plaques and soluble oligomers in high-order association brain regions. The presence of intracellular neurofibrillary tangles, neuroinflammation, neuronal dysfunction and death further characterizes this disease. Mounting evidence suggests that Aβ plays a critical early role in AD pathogenesis, and the basic tenant of the amyloid (or Aβ cascade) hypothesis is that Aβ aggregates trigger a complex pathological cascade which leads to neurodegeneration [1]. A strong genetic correlation exists between FAD and the 42 amino acid Aβ form (Aβ42; reviewed in [2-4]). Aβ is derived from APP and mutations in APP and PS increase Aβ42 production and cause FAD with nearly 100% penetrance. Down's syndrome (DS) patients, who have an extra copy of the APP gene on chromosome 21, and FAD families with a duplicated APP gene locus [5], exhibit total Aβ overproduction and all develop early-onset AD. In FAD, the Aβ42 increase is present years before AD symptoms arise, suggesting that Aβ42 is likely to initiate AD pathophysiology. The robust association of Aβ42 overproduction with FAD argues strongly in favor of a critical role for Aβ42 in the etiology of AD, including in SAD. Fibrillar and oligomeric forms of Aβ appear neurotoxic *in vitro* and *in vivo*. Importantly, in specific transgenic (Tg) mouse models of AD the lack of Aβ correlates with the absence of neuronal loss and improved cognitive function [6-8]. Such data provides direct evidence for the amyloid hypothesis *in vivo*, and also indicates that Aβ is directly responsible for neuronal death. Consequently, strategies to lower Aβ42 levels in the brain are anticipated to be of therapeutic benefit in AD.

Aβ peptide is generated following the sequential cleavage of APP by *β*- and *γ*-secretase in the amyloidogenic pathway [9, 10]. Aβ genesis may be precluded if APP is cleaved by α-secretase within the Aβ domain in the non-amyloidogenic pathway (see Fig. **1**). Recently, the secretases have been identified and the *β*-secretase is known to be *β*-site APP cleaving enzyme I (BACE1) [11-14], a novel aspartyl protease. BACE1 cleavage of APP is a pre-requisite for Aβ formation. Aβ genesis is initiated by BACE1 cleavage of APP at the Asp+1 residue of the Aβ sequence to form the N-terminus of the peptide. This scission liberates two cleavage fragments: a secreted APP ectodomain, APPsβ and a membrane-bound carboxyl terminal fragment (CTF). In many instances, an increase in non-amyloidogenic APP metabolism is coupled to a reciprocal decrease in the amyloidogenic processing pathway, and vice-versa, as the *α*- and *β*-secretase moieties compete for APP substrate [10, 13]. In the case of *γ*-secretase is a multi-subunit protease complex, itself an integral membrane protein, those cleaves single-pass transmembrane proteins at residues within the transmembrane domain. The most well-known substrate of gamma secretase is amyloid precursor protein, a large integral membrane protein that, when cleaved by both gamma and beta secretase, produces a short 39-42 amino acidpeptide called amyloid beta whose abnormally folded fibrillar form is the primary component of amyloid plaques found in the brains of Alzheimer's disease patients. Gamma secretase is also critical in the related processing of the Notch protein [15, 16].

*Address correspondence to this author at the Department of Organic Chemistry, University of Santiago de Compostela, Spain;
Tel: + 34 881814985; E-mail: francisco.prado@usc.es

1875-5607/12 $58.00+.00

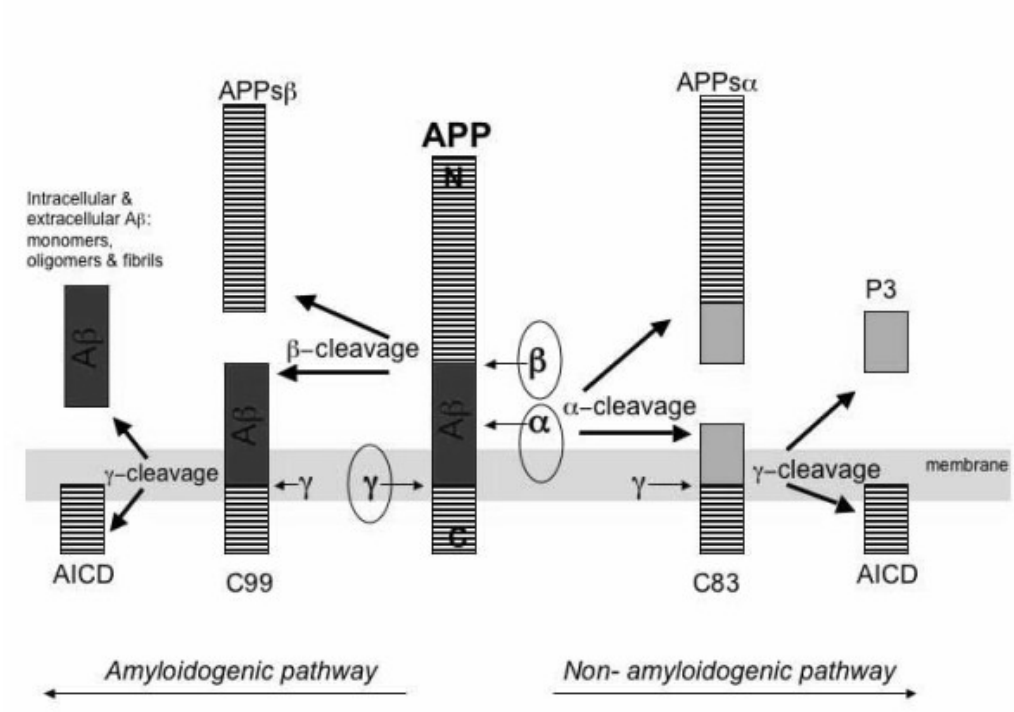

Fig. (1). APP metabolism by the secretase enzymes.

Given that both secretase are the initiating enzyme in Aβ generation, and putatively rate-limiting, it is considered a prime drug target for lowering cerebral Aβ levels in the treatment and/or prevention of AD. Prior to its identification, numerous studies were undertaken to define the characteristics of *β*-secretase activity. Although the majority of body tissues exhibit *β*-secretase activity [17], highest activity levels were observed in neural tissue and neuronal cell lines [18]. Indeed, *β*-secretase appeared to predominate in neurons, with the level of *β*-secretase activity appearing lower in astrocytes [19]. Data showing that *β*-secretase efficiently cleaved only membrane-bound substrates [20] indicated that the enzyme was likely membrane-bound or closely associated with a [21] prevent the buildup of beta-amyloid and may help slow or stop the disease However, current AD therapies are merely palliative and only temporarily slow cognitive decline, and treatments that address the underlying pathologic mechanisms of AD are completely lacking.

In the last years, a number of publications have appeared suggesting GSK-3 as a target for the treatment of AD. Two isoforms of GSK-3 exists, GSK-3*α* and GSK-3*β*, both share a high homology at their catalytic site but the *α* form possess an extended N-terminus with respect to the *β* form [22, 23]. The phosphorylation of proteins by GSK-3 is an important link in neural function [24-26]. Two are the characteristic neuropathological hallmarks of AD, Neurofibrillary Tangles (NFT´s) and increase production of amyloid beta (Aβ) peptides, where NFT´s are composed of highly phosphorylated form of the microtubule associated protein tau [27] and studies have shown that GSK-3 is one of the main *in vivo* players of phosphorylation of tau protein [28]. It has been reported that Lithium, a GSK-3 inhibitor, block production of Aβ peptides by interfering with APP cleavage at *γ*-secretase step, where the target for Lithium is GSK-3*α* [21, 22]. Phiel *et al.* [21] showed that selective reduction in concentration of the *α* isoform led to a decrease in the concentration of Aβ40 and Aβ42, primary constituents of amyloid plaques in AD. Thus inhibition of GSK-3*α* could potentially provide dual therapy against AD, preventing the buildup of amyloid plaques and of neurofibrillary tangles [21, 29, 30].

GSK-3*β* is a serine/threonine kinase and is thought to be a key factor for aberrant tau phosphorylation [31]. Activated GSK-3*β* coexists with progression of NFT´s and neurodegeneration in the AD brain [32-34]. A conditional GSK-3*β* overexpressing transgenic mouse exhibits persistent tau hyperphosphorylation, pretangle-like somatodendritic localization of tau, neuronal death in hippocampus and cognitive deficits [35, 36]. These studies suggest that GSK-3*β* is associated with AD progression, and GSK-3*β* inhibition is expected to be a promising therapeutic approach for AD.

In this sense, quantitative structure-activity relationships (QSAR) could play an important role in studying these *β* and *γ*-secretase inhibitors. QSAR models are necessary in order to guide the *β* and *γ*-secretase inhibitors.

On the other hand, QSAR models can be used to explore the relationships between the structural spaces of compounds as inhibitors for specific enzymes, such as MAO inhibitors [37], HIV-1 integrase inhibitors [38], and/or protease inhibitors [39] or tyrosinase inhibitors [40-42]. In fact, Almost all QSAR techniques are based on the use of molecular descriptors, which are numerical series that codify useful chemical information and enable correlations between statistical and biological properties [43, 44]. Recently, the

field has moved from small molecules to proteins and other systems. For instance, González-Díaz *et al*. discussed the use of these methods but only from the point of view of proteins [45]. Later, some groups published different papers in one special issue on QSAR but also restricted to the field of protein and proteomics [46-52]. In other recent issue, guest-edited by González-Díaz [53] appeared a series of papers devoted to QSAR/QSPR techniques for low-molecular-weight drugs [53-62]. Most recently, Prado-Prado *et al*. [63] published a mt-QSAR for anti-parasitic drugs. This year was published other issue [64] focused on QSAR/QSPR models and graph theory used to approach Drug ADMET processes and Metabolomics [65-72]. Last, one of the most recent issues published is devoted to discuss the applications of QSAR in Pharmaceutical Design [73-82]. In the present work, we firstly revised the state-of-art on the design, synthesis, and biological assay of *β* and *γ*-secretase inhibitors. Next, we review previous works based on 2D-QSAR, 3D-QSAR, CoMFA, CoMSIA and docking techniques, which studied different compounds to find out the structural requirements. The topics reviewed, discussed, and/or reported in this paper are:

1. **Studies of *γ*-secretase inhibitors**
   - ***1.1. Synthesis and Theoretical studies of γ-secretase inhibitors***
   - ***1.2. Design and synthesis of pyridine derivatives as BACE-1 inhibitors***
   - ***1.3. Discover non-peptide inhibitors of BACE-1 using VHTS***
   - ***1.4. Distinct Pharmacological Effects of Inhibitors of γ-secretase***
   - ***1.5. 3D-QSAR studies of γ-secretase inhibitors***
   - ***1.6. MD simulations of Aβ fibril interactions***
2. **Studies of *β*-secretase inhibitors**
   - ***2.1. Synthesis, Theoretical studies and Biological Assay of β-secretase inhibitors***
   - ***2.2. Models of novel pyridinium-based potent β-secretase inhibitory leads***
   - ***2.3. CoMFA & CoMSIA of hydroxyethylamine derivatives as BACE-1 inhibitors***
   - ***2.4. Virtual Screening and Protonation States at Asp32 and Asp228***
   - ***2.5. Docking scoring function based on 2D-descriptors***
   - ***2.6. Induced-Fit Docking of Peptidic and Pseudo-peptidic BACE-1 inhibitors***
3. **Studies of GSK-3*α* inhibitors**
   - ***3.1. 2D-QSAR for 3-anilino-4-phenylmaleimides***
   - ***3.2. 3D-QSAR and docking of 3-anilino-4-phenylmaleimides***
   - ***3.3. QSAR studies of Some GSK-3α Inhibitory pyrimidines***
4. **Studies of GSK-3*β* inhibitors**
   - ***4.1. Design, synthesis and SAR of oxadiazole derivatives***
   - ***4.2. Linear/Nonlinear Regression Methods for Prediction of Glycogen***
   - ***4.3. Molecular modeling, docking and 3D-QSAR studies for maleimides***
   - ***4.4. Molecular docking and biological testing of inhibitors of GSK-3β***
   - ***4.5. 3D-QSAR Modelling of Paullones***
   - ***4.6. Modeling of Binding Mode of Benzo[e]isoindole-1,3-diones***

DISCUSSION

QSAR and Theoretical Studies for Neurodegene Inhibitors

In this section we updated the contents presented in our recent review published in Current Drugs Metabolism [83]. The high number of possible candidates to *β*-secretase inhibitors creates the necessity of Quantitative Structure-Activity Relationship models in order to guide the *β*-secretase inhibitor synthesis. In this work, we revised different computational studies for a very large and heterogeneous series of *β*-secretase. First, we revised QSAR studies with conceptual parameters. Next, using method of regression analysis; and QSAR studies in order to understand the essential structural requirement for binding with receptor. Next, we review 3D QSAR, CoMFA and CoMSIA with different compound to find out the structural requirements for *β*-secretase inhibitors.

1. Studies of γ-Secretase Inhibitors

1.1. Design and Synthesis of Pyridine Derivatives as BACE-1 Inhibitors

Soo-Jeong Choi, *et al*. [84], had designed and synthesized of 1,4-dihydropyridine derivatives as BACE-1 inhibitors using a 1,4-dihydropyridine (DHP) scaffold. They had synthesized new inhibitors of BACE-1 (the protein that has been shown to be an attractive therapeutic target in Alzheimer's disease) by modifying the known BACE inhibitor 2 containing a hydroxyethylamine (HEA) motif, see Fig. (**2**). Using structure-based drug design based on computer-aided molecular docking, the isophthalamide ring was replaced with a 1,4-dihydropyridine ring as a brain-targeting strategy. After their synthesis, the dihydropyridine derivatives were evaluated their BACE-1-inhibitory activities using a cell-based, reporter gene assay system that measures the cleavage of alkaline phosphatase (AP)-APP fusion protein by BACE-1.

Molecular modeling was performed using CDOCKER, a CHARMm based molecular dynamics docking algorithm Discovery Studio 2.0 (Accelrys). The BACE-1 structure co-crystallized was obtained from the PDBdata bank (PDB code: 2B8L). A protein clean process and a CHARMm-force field were sequentially applied. The area around 2 was chosen as the active site, with the radius set as at 8-A. After removing 2 from the structure of the complex, a binding sphere in the three axis directions was constructed around the active site. Al default parameters were used in the docking process. CHARMm based molecular dynamics (1000 steps) were used to generate random ligand

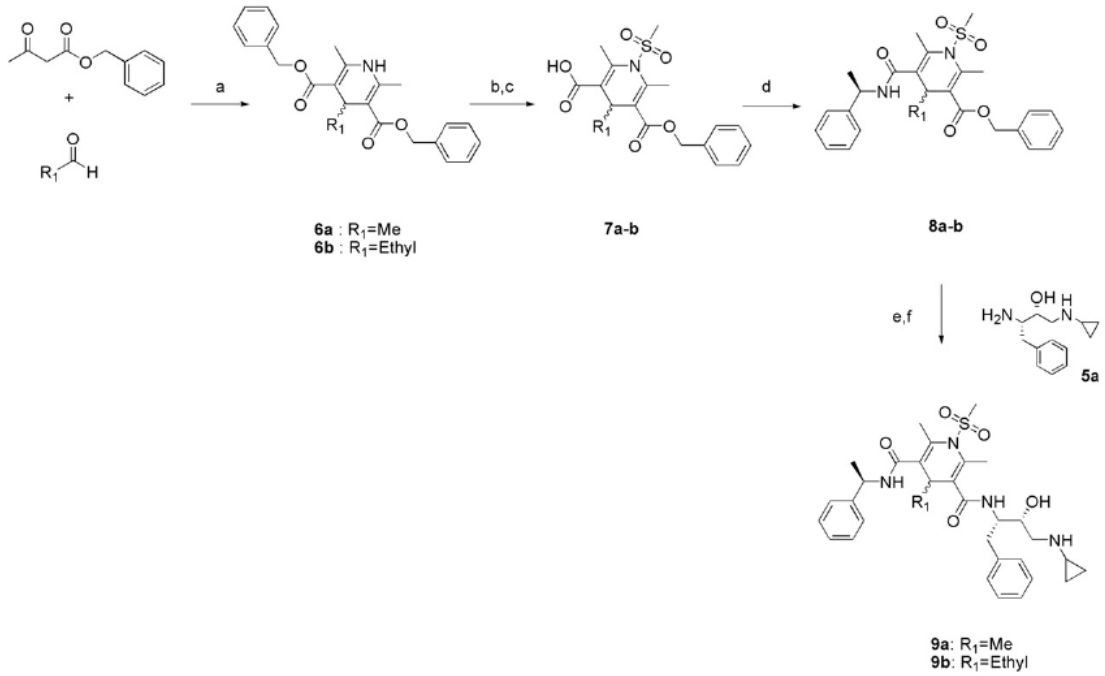

Fig. (2). Synthesis of 1-methylsulfonamide-2,6-dimethyl-1,4-dihydropyridine derivatives.

Reagent: (**a**) NH_4OAc, Ethanol, 90 ºC, 24 h, 98%; (**b**) Methane sulfonylchloride, NaH, DMF, 0-60 ºC, 4 h, 35%; (**c**) $AlCl_3$, Anisole, DCM, -50 ºC to RT, 2 h, 21%; (**d**) R-methylbenzylamine, PyBOP, DIPA, DCM, 1 h, 70%; (**e**) AlCl3, Anisole, DCM, 50 C to RT, 2 h, 30%; (**f**) Compound 5a, PyBOP, DIPEA, DCM, 15 min, 65%.

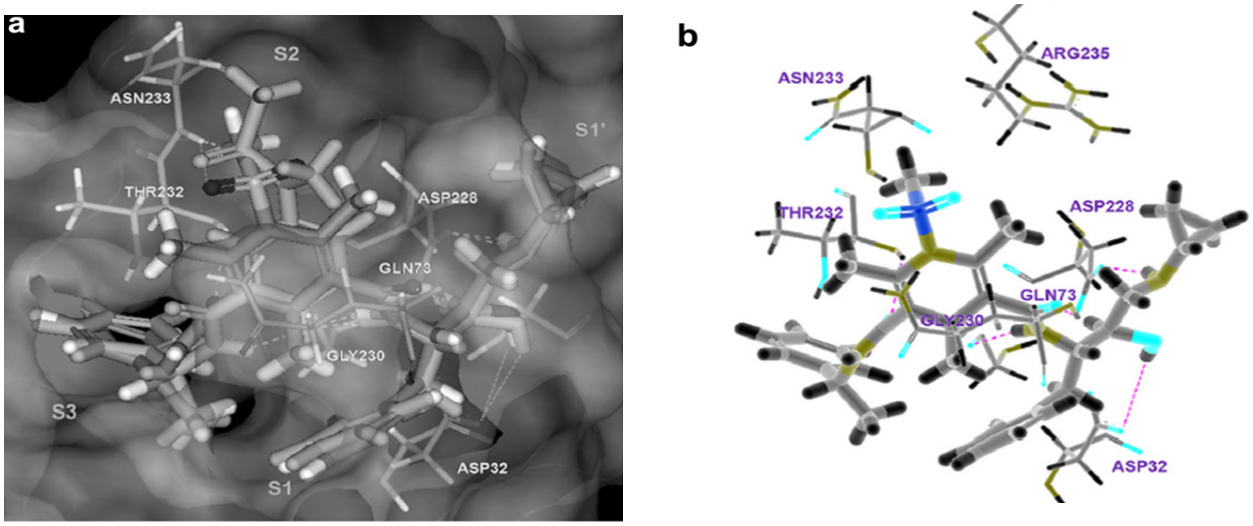

Fig. (3). Overlay of inhibitor 2 (green) and inhibitor **9a** in the BACE-1 active site, b. Interactions of **9a** in the active site of BACE-1-Hydrogen bonds are shown with dotted lines (For interpretation of the references to color in this figure legend, the reader is referred to the web version of this article).

conformations and the position of any ligand was optimized in the binding site using rigid body rotation followed by simulated annealing at 700 K. Final energy minimization was set as the full potential mode. The final binding conformation was determined on the basis of energy (see Fig. **3**).

Based on molecular docking results, we designed 1,4-DHP derivatives as BACE-1 inhibitors using five strategies. These were replacement of the bulky a-methylbenzamide group in 2 with a benzyl ester or smaller acetyl group for binding in the S3 pocket; modification of the sulfonamide group in the aromatic scaffold of 2 with alkyl ester or amide groups, maintaining the important hydrogen bonding with Asn233 in the S2 binding pocket; incorporation of additional hydrophobic interactions into the S1 binding pocket by introduction of alkyl or aryl groups, including methyl, ethyl,

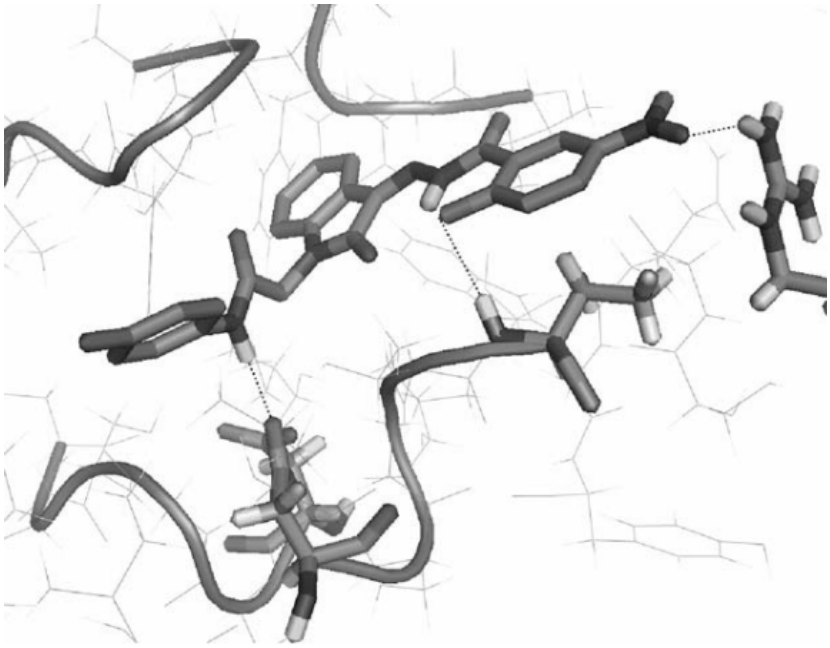

Fig. (4). Binding pose of 1 (corresponding to conformer 20) in the BACE-1 active site generated using AutoDock.

propyl, isopropyl, and phenyl groups; alteration of the cyclopropyl group at the R4 position to other aromatic groups, thus changing hydrophobic interactions in the S20 binding pocket by extension toward the prime-side of the enzyme; and, alterations at the 2 and 6 positions of the 1,4-DHP scaffold by synthesis of 2-monomethyl and 2,6-unsubstituted analogs.

Their results show that most of the 1,4-DHP analogs showed BACE-1-inhibitory activities with IC_{50} values in the range 8e30 mM, suggesting that the 1,4-DHP skeleton may be utilized to develop brain-targeting BACE-1 inhibitors.

1.2. Discover Non-Peptide Inhibitors of BACE-1 Using VHTS

A novel series of isatin-based inhibitors of b-secretase (BACE-1) using a virtual highthroughput screening approach have identified by Moka *et al*. [85]. Structure-activity relationship studies revealed structural features important for inhibition. Docking studies suggest these inhibitors may bind within the BACE-1 active site through H-bonding interactions involving the catalytic aspartate residues.

They used AutoDock to separately dock the two proposed favored conformations 19 and 20 of compound 1 into the active site of BACE-1 (PDB code 1M4H). While the docking of conformer 19 did not give any solutions consistent with the observed biological activity, docking of conformer 20 revealed a binding pose which was consistent with the observed activities of compounds 1-8 (see Fig. **4**).

This figure shows the lowest-energy binding pose identified for conformer 20 within BACE-1. It is noteworthy that an analogous binding pose was also identified using eHiTS. The acetamide moiety is predicted to occupy the catalytic site, with the acetamide N-H acting as an H-bond donor to the catalytic residue Asp228 (H-bond length = 1.86 ÅA 0).

The phenol unit is predicted to make an H-bond contact with the backbone nitrogen of Thr232 (H-bond length = 2.20 ÅA 0) and to partly occupy the P2 substrate pocket. This feature implies the phenol might be involved in both the formation of the intermolecular H-bonding network, and also in intermolecular H-bonding interactions with the enzyme. The nitro group in 1 is predicted to extend into the P4 pocket, possibly participating in weak H-bonding with the side chain of Arg307 (H-bond length = 2.13 ÅA 0), consistent with the slight decrease in the binding affinity exhibited by compound.

In summary, the authors, using the virtual high-throughput screening software eHiTS, have discovered a novel non-peptidic inhibitor of BACE-1 based on an isatin motif. Studies of the biological activity of structural variants in combination with in silico docking suggest the inhibitor adopts a planar conformation, which is stabilized by intramolecular H-bonding from the phenolic moiety. Additionally, binding to BACE-1 appears to involve H-bonding interactions between the p-tolylamide of 1 and the catalytic residue Asp228.

A recent report detailing the discovery of a series of potent small molecule BACE-1 inhibitors compares the ligand efficiency (LE) of a range of reported inhibitors of BACE-1. In this study, the authors noted that despite the high potency of the previously reported peptide-based BACE-1 inhibitors such as OM99-2 (K_i = 1.6 nM), the relatively high molecular weights of these systems (e.g., OM99-2 has a molecular weight of 893) often result in them having relatively poor ligand efficiency (e.g., LE = 0.19 for OM99-2). For this study, although still somewhat below the preferred minimum value of LE = 0.3, compound 1 (molecular weight = 461) has LE = 0.22 and therefore, is closer to the preferred value than the potent but considerably larger peptidic inhibitors reported previously. They have demonstrated that eHiTS is a powerful screening tool to

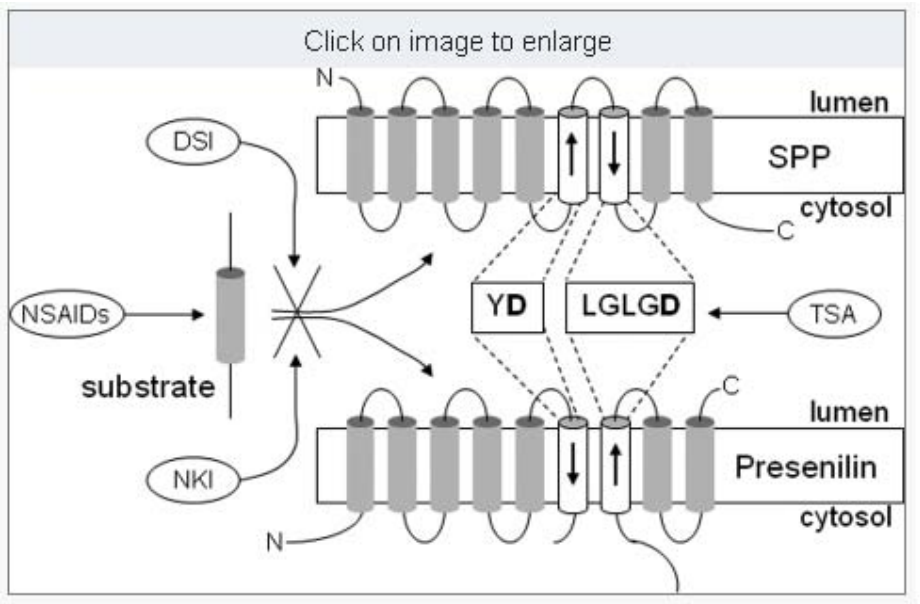

Fig. (5). Schematic mechanisms of inhibitor. Transition-state analogue (TSA) inhibitor targets the active site, and helical peptide docking site inhibitor (DSI) prevents initial substrate interaction with the protease. NSAIDs target the substrate, and naphthyl ketone inhibitors (NKI) disrupt the initial interaction between substrate and protease (selectively for APP in the case of ɣ-secretase).

identify biologically active compounds quickly and efficiently.

1.3. Distinct Pharmacological Effects of Inhibitors of γ -Secretase

T. Sato, *et al*. [86], have report that helical peptide inhibitors designed to mimic SPP substrates and interact with the SPP initial substrate-binding site (the "docking site") inhibit both SPP and *γ*-secretase, but with submicromolar potency for SPP. SPP was labeled by helical peptide and transition-state analogue affinity probes but at distinct sites. Nonsteroidal anti-inflammatory drugs, which shift the site of proteolysis by SPP and *γ*-secretase, did not affect the labeling of SPP or *γ*-secretase by the helical peptide or transition-state analogue probes. On the other hand, another class of previously reported *γ*-secretase modulators, naphthyl ketones, inhibited SPP activity as well as selective proteolysis by *γ*-secretase. These naphthyl ketones significantly disrupted labeling of SPP by the helical peptide probe but did not block labeling of SPP by the transition-state analogue probe. With respect to *γ*-secretase, the naphthyl ketone modulators allowed labeling by the transition-state analogue probe but not the helical peptide probe. Thus, the naphthyl ketones appear to alter the docking sites of both SPP and *γ*-secretase. These results indicate that pharmacological effects of the four different classes of inhibitors (transition-state analogues, helical peptides, nonsteroidal anti-inflammatory drugs, and naphthyl ketones) are distinct from each other, and they reveal similarities and differences with how they affect SPP and *γ*-secretase (see Fig. **5**).

1.4. 3D-QSAR studies of γ-secretase inhibitors

A 3D-QSAR analysis on a series of 67 benzodiazepine analogues reported as *γ*-secretase inhibitors using molecular field analysis (MFA), with G/PLS to predict steric and electrostatic molecular field interaction for the activity have performed by T. Sammi *et al.* [87].

The MFA study was carried out using a training set of 54 compounds. The predictive ability of model developed was assessed using a test set of 13 compounds (r^2_{pred} as high as 0.729). The analyzed MFA model has demonstrated a good fit, having r^2 value of 0.858 and cross validated coefficient, r^2_{cv} value as 0.790. The analysis of the best MFA model provided insight into possible modification of the molecules for better activity.

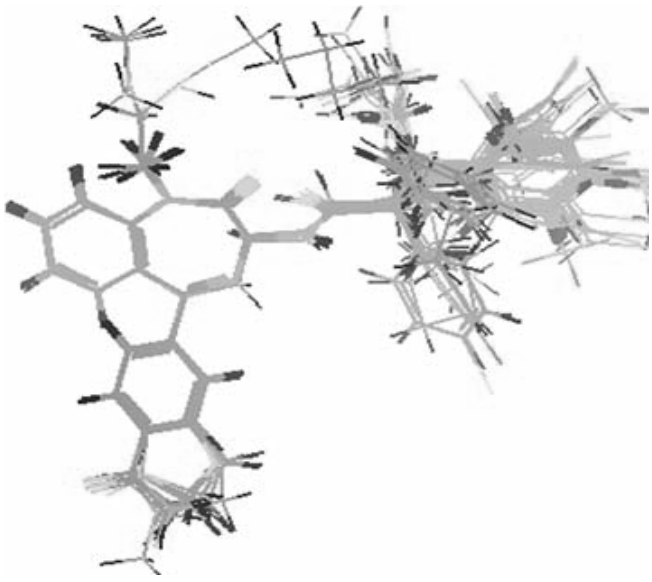

Fig. (6). Stereoview of all the aligned molecules.

To obtain effective 3D-QSAR models the method that they used for performing the alignment was the maximum common subgroup (MCSG). This method looks at molecules

Table 1. Various Statistical Parameters Along with their Numerical Value Obtained for the Best Model

	Parameter	Value
1.	Data points (n)	54
2.	Square of correlation coefficient (r^2) for training set	0.858
3.	Leave one out cross validated correlation coefficient (r^2_{cv})	0.790
4.	Predicted sum of squares (PRESS)	16.086
5.	Number of PLS components (C)	5
6.	Simple correlation coefficient (r^2_{pred}) for test set	0.729
7.	Predicted correlation coefficient (r^2_{pred})	0.685
8.	Bootstrap correlation coefficient (r^2_{bs})	0.843
9.	Lest Square error (LSE)	0.208
10.	Predicted root mean square error ($RMSE_{pred}$)	0.579
11.	Slope of regression line of observed vs predicted activity passing through origin(k)	1.004
12.	Slope of regression line of predicted vs observed activity passing through origin(k')	0.987
13.	Correlation coefficient for regression line of observed vs predicted activity passing through origin(R2 0)	0.999
14.	Correlation coefficient for regression line of predicted vs observed activity passing through origin	0.998

[a]Correlation coefficient calculated using Eq. 3.

as points and lines, and uses the techniques of graph theory to identify patterns. It finds the largest subset of atoms in the shape reference compound that is shared by all the structures in the data set and uses this subset for alignment. A rigid fit of atom pairing was performed to superimpose each structure so that it overlays the shape reference compound. The most active bold-faced portion of molecule 1, was used as the template for the superposition (see Fig. **6**).

G/PLS technique available in QSAR environment of Cerius2 software was used to perform regression analysis of data. As there were large numbers of points used as independent variables, genetic partial least squares (G/PLS) were used to derive QSAR models. G/PLS is derived from two QSAR calculation methods: Genetic function approximation (GFA) and partial least squares (PLS). The GFA algorithm approach builds multiple models rather than single model; it automatically selects which features are to be used in model. Further it is better at discovering combinations of features that take advantage of correlations between multiple features. In PLS, variables might be overlooked during interpretation or in designing the next experiment even though cumulatively they are important. It gives a reduced solution, which is statistically more robust than multiple linear regressions (MLA). The linear PLS model finds "new variables" (latent variables or X scores) which are linear combinations of original variables. To avoid over fitting, a strict test for the significance of each consecutive PLS component is necessary and then stopping when the components are non-significant. Cross validation a practical and reliable way of testing this significance. G/PLS combines the best features of GFA and PLS. In GFA; equation models have a randomly chosen proper subset of independent variables. As a result of multiple linear regressions (MLA) on each model, the best ones become the next generation and two of them produce an offspring. This was repeated 50,000 (default, 5000 times). For other settings, all defaults were used. Application of G/PLS thus allows the construction of large QSAR equations while still avoiding over fitting and eliminating most variables. The best model was selected on statistical measures such as data points (n), square correlation coefficient (r^2), cross-validated correlation coefficient (r^2_{cv}), predicted correlation coefficient (r^2_{pred}), predicted sum of squares (PRESS), bootstrap correlation coefficient (r^2_{obs}) (see Table **1**).

1.5. MD Simulations of Aβ Fibril Interactions

N.J. Brucea, *et al.*, use molecular dynamics simulations to compare the model of interaction of an active (LPFFD) and inactive (LHFFD) β-sheet breaker peptide with an Aβ fibril structure from solid-state NMR studies. This study is based in the matter that have accumulation and aggregation of the 42-residue amyloid-β (Aβ) protein fragment, which originates from the cleavage of amyloid precursor protein by *β* and *γ* secretase, correlates with the pathology of Alzheimer's disease (AD). Possible therapies for AD include peptides based on the Aβ sequence, and recently identified small molecular weight compounds designed to mimic these, that interfere with the aggregation of Aβ and prevent its toxic effects on neuronal cells in culture. Here, they found that LHFFD had a weaker interaction with the fibril than the active peptide, LPFFD, from geometric and energetic considerations, as estimated by the MM/PBSA approach. Cluster analysis and computational alanine scanning identified important ligand-fibril contacts, including a possible difference in the effect of histidine on ligand-fibril π-stacking interactions, and the role of the proline residue in establishing contacts that compete with those essential for maintenance of the inter-monomer β-sheet structure of the

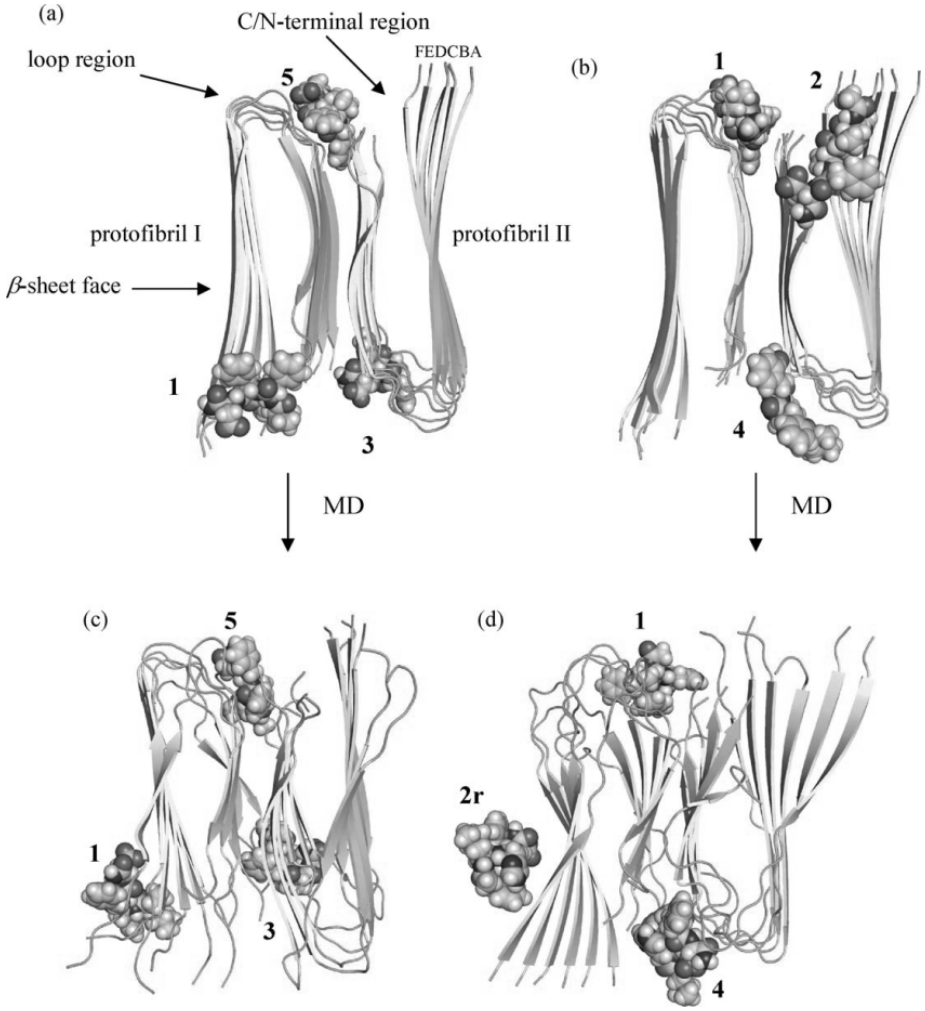

Fig. (7). Comparison of docked poses of (**a**) active peptide LPFFD (**b**) inactive peptide LHFFD; and comparison of MD-refined poses of (**c**) active peptide LPFFD and (**d**) inactive peptide LHFFD.

fibril. Their results show that molecular dynamics simulations can be a useful way to classify the stability of docking sites. These mechanistic insights into the ability of LPFFD to reverse aggregation of toxic Aβ will guide the redesign of lead compounds, and aid in developing realistic therapies for AD and other diseases of protein aggregation (see Fig. **7**).

2. Studies of β*-Secretase Inhibitors*

2.1. Models of Novel Pyridinium-Based Potent β*-Secretase Inhibitory Leads*

In one article by Al-Nadaf *et al.* [88] explore the pharmacophoric space of 129 known BACE inhibitors have potential as anti-Alzheimer's disease treatments. The QSAR analysis employed to select optimal combination of pharmacophoric models and 2D physicochemical descriptors capable of explaining bioactivity variation (r^2 = 0.88, F = 60.48, r^2_{LOO} = 0.85, r^2_{PRESS} against 25 external test inhibitors = 0.71). They were obliged to use ligand efficiency as the response variable because the logarithmic transformation of bioactivities failed to access self-consistent QSAR models. The authors constructed three pharmacophoric models emerged in the successful QSAR equation suggesting at least three binding modes accessible to ligands within BACE binding pocket. The QSAR equation and pharmacophoric models were validated through ROC curves (see Table **2**),

Table 2. ROC[a] Performances of QSAR-Selected Pharmacophores as 3D Search Queries

Pharmacophore	ROC[a]/AUC[b]	ACC[c]	SPC[d]	TPR[e]	FNR[f]
Hypo10/10	0.982	0.961	0.988	0.28	0.011345
Hypo6/18	0.981	0.961	0.975	0.6	0.024311
Hypo1/21	0.738	0.961	0.9611	0.96	0.038898

[a]ROC: receiver operating characteristic, [b]AUC: area under the curve, [c]ACC: overall accuracy, [d]SPC: overall specificity, [e]TPR: overall true positive rate, [f]FNR: overall false negative rate.

and were employed to guide synthesis of novel pyridinium-based BACE inhibitors.

2.2. CoMFA & CoMSIA of Hydroxyethylamine Derivatives as BACE-1 Inhibitors

Pandey *et al.* [89] were developed three-dimensional quantitative structure-activity relationship (3D-QSAR) models based on comparative molecular field analysis (CoMFA) and comparative molecular similarity indices analysis (CoMSIA), on a series of 43 hydroxyethylamine derivatives, acting as potent inhibitors of β-site amyloid precursor protein (APP) cleavage enzyme (BACE-1). They used a crystal structure of the BACE-1 enzyme (PDB ID: 2HM1) with one of the most active compound presented in this paper was available, and we assumed it to be the bioactive conformation of the studied series, for 3D-QSAR analysis. Statistically significant 3D-QSAR model was established on a training set of 34 compounds, which were validated by a test set of 9 compounds. For the best CoMFA model, the statistics are, $r^2 = 0.998$, $r^2_{cv} = 0.810$, $n = 34$ for the training set and $r^2_{pred} = 0.934$, $n = 9$ for the test set. For the best CoMSIA model (combined steric, electrostatic, hydrophobic, and hydrogen bond donor fields), the statistics are $r^2 = 0.978$, $r^2_{cv} = 0.754$, $n = 34$ for the training set and $r^2_{pred} = 0.750$, $n= 9$ for the test set, see Table **3**. The resulting contour maps, produced by the best CoMFA and CoMSIA models, were used to identify the structural features relevant to the biological activity in series of analogs. The data generated from the present study will further help to design novel, potent, and selective BACE-1 inhibitors.

Table 3. PLS Summary of CoMFA and CoMSIA Results

Statistical parameters	CoMFA (S E)	CoMSIA (S EHD)
Number of molecules in training set	34	34
Number of molecules in test set	9	9
r^2 cv	0.810	0.754
NOC	7	4
SEE	0.063	0.204
r^2	0.998	0.978
F-test	2009.08	324.673
r^2_{bs}	0.999	0.989
SD_{bs}	0.001	0.006
r^2_{pred}	0.934	0.750
Percentage of field contributions		
S	47.4	24.8
E	52.6	34.0
H	–	26.3
D	–	14.9

Abbreviations: S (steric field), E (electrostatic field), H (hydrophobic field), D (hydrogen bond donor field) r^2_{cv} =Cross-validated correlation coefficient by PLS LOO method, NOC=Optimum number of components as determined by PLS LOO cross-validation study, SEE=Standard error of estimate, r^2 =Conventional correlation coefficient, r^2_{bs} =Correlation coefficient after 100 runs of boot strapping, SD_{bs} =Standard deviation from 100 runs of bootstrapping, r^2_{pred} =Predictive correlation coefficient.

2.3. Virtual Screening and Protonation States at Asp32 and Asp228

M. Keseru *et al.* [90] performed a comparative virtual screen for β-secretase (BACE1) inhibitors using different docking methods (FlexX and FlexX-Pharm), scoring functions (Dock, Gold, Chem, PMF, FlexX), protonation states (default and calculated), and protein conformations (apo and ligand bound). Apo and ligand bound conformations of BACE1 were both found to be suitable for virtual screening. Assigning calculated protonation states to catalytic Asp32 and Asp228 residues resulted in significant improvement of enrichment factors as calculated at 1% of the ranked database. The authors used 1FKN to obtain no enrichment by FlexX/D-Score that was improved to ligand when considering calculated protonation states. They also show that combining calculated protonation states with pharmacophore constraints using FlexX-Pharm/D-Score improved enrichment further to ligand. Enrichments reported in this study suggest our screening protocol will be effective in the virtual screening of large compound libraries for BACE1 inhibitors.

2.4. Docking Scoring Function Based on 2D-Descriptors

In this paper Hetényi [91] showed a key step in the molecular engineering of such potent lead compounds is the prediction of the energetics of their binding to the macromolecular targets. Although sophisticated experimental and in silico methods are available to help this issue, the structure-based calculation of the binding free energies of large, flexible ligands to proteins is problematic. In this study, a fast and accurate calculation strategy is presented; following modification of the scoring function of the popular docking program package AutoDock and the involvement of ligand based two-dimensional descriptors. Quantitative structure-activity relationships with good predictive power were developed. The best results of this paper were shown in Table **4**. Thorough cross-validation tests and verifications were performed on the basis of experimental binding data of biologically important systems. The capabilities and limitations of the ligand based descriptors were analyzed. According to the authors the application of these results in the early phase of lead design will contribute to precise predictions, correct selections, and consequently a higher success rate of rational drug discovery.

2.5. Induced-Fit Docking of Peptidic and Pseudo-Peptidic BACE-1 Inhibitors

Inhibition of β-secretase (BACE 1) has recently been investigated as a promising therapeutic approach in the treatment of Alzheimer's disease, and a growing number of BACE 1 inhibitors and crystal structures of BACE 1/inhibitors complexes have been reported. Moitessier *et al.* [92] report herein a predictive computational method and its application to potential BACE 1 inhibitors. Using a training set of 50 known highly flexible inhibitors, they developed a docking method that accounts for the flexibility of both the protein and the inhibitors. Protein flexibility is accounted for using a specifically designed genetic algorithm. In this paper developed a scoring function consisting of force field

Table 4. The Results Produced by the Best CoMFA and CoMSIA Models

QSAR	descriptor (Di)							
		coefficient (Ri)	error of coeff.	t-value	R^2	R^2_{cv}	s^2	F-value
A	1	¢GTH	3.1216 × 10-1	2.4686 × 10-2	0.799	0.774	1.05	93.36
	2	RPCGEN	3.2582 × 101	6.9963				
		constant	-4.1980	6.9930 × 10-1				
B	1	¢GTH	2.7077 × 10-1	2.2926 × 10-2	0.859	0.838	0.76	93.17
	2	RPCGEN	5.7129 × 101	8.1307				
	3	J	-6.2410 × 10-1	1.4148 × 10-1				
		constant	-4.6864	6.0281 × 10-1				

Standard deviations (s^2), squares of the correlation coefficients (R^2), and leave-one-out cross-validated correlation coefficients (R^2_{cv}) of the regressions are tabulated.

evaluation of the inhibitor/protein interactions and two additional terms for hydrogen bonding and entropy change upon binding. Discarding three outliers from the training set, the protocol was found to perform well with an rmsd of 1.19 kcal/mol and r^2 value of 0.789. Evaluation of the predictive power was carried out by virtual screening of 80 synthetic compounds. The significant enrichment at the top of the ranking list in active compounds demonstrated the ability of the docking and scoring protocol to rank the compounds relative to their activities.

3. Studies of GSK-3α Inhibitors

3.1. 2D-QSAR for 3-anilino-4-phenylmaleimides

In this paper, Sivaprakasam *et al.* [30] reported a 2D-QSAR exploration of the physicochemical (hydrophobic, electronic, and steric) and structural requirements among 3-anilino-4-phenylmaleimides toward GSK-3*α* binding. Using Fujita-Ban and Hansch QSAR analysis, electronic and steric interactions at the 4-phenyl ring and hydrophobic interactions at the 3-anilino ring were shown to be crucial. Hansch type QSAR was still widely used in the lead optimization stage of synthetic and other projects.

Fujita-Ban analysis of 3-anilino-4-phenylmaleimides revealed that certain structural features such as Cl, OCH3, and NO2 mono substitution at any position around the 4-phenyl ring were favorable for GSK-3*α* inhibition. Substituents at the 3-anilino ring such as 3-Cl, 4-Cl, 5-Cl, 3-COOH, 4-OH, and 4-SCH3 were positively and 3-OH was negatively correlated with GSK-3*α* inhibitory activity.

Through Hansch QSAR analyses, they found that the GSK-3*α* inhibitory activity was enhanced by: 1. Electron-withdrawing, bulky *ortho* substituents at 4-phenyl ring; 2. 4-chloro substitution around anilino ring; 3. 3-anilino rather than 3-N-methylanilino derivatives; 4. Hydrophobic *meta* substituents on the anilino ring. Overall, QSAR models 13a and 14a suggested electronic and steric effects at the 4-phenyl ring and hydrophobic effects at the 3-anilino or 3-N-methylanilino ring were crucial. Their 2D-model (Fig. **8**) illustrated these effects which are essential for binding of the maleimides to the GSK-3*α* enzyme. Their analysis had provided key information regarding ligand–target interactions which they believed will help medicinal chemists to design more potent GSK-3*α* inhibitors.

3.2. 3D-QSAR and Docking of 3-anilino-4-phenylmaleimides

In this article [93] was reported 3D-QSAR analyses using CoMFA and CoMSIA and molecular docking studies on 3-anilino-4-phenylmaleimides as GSK-3*α* inhibitors, in order to better understand the mechanism of action and structure-activity relationship of these compounds. Comparison of the active site residues of GSK-3*α* showed that all the key amino acids involved in polar interactions with the maleimides for the *β* isoform were the same in the *α* isoform, except that Asp133 in the *β* isoform was replaced by Glu196 in the *α* isoform. They prepared a homology model for GSK-3*α*, and showed that the change from Asp to Glu should not affect maleimide binding significantly. Our best CoMFA model contained steric and electrostatic fields and had $n = 56$, $q^2 = 0.844$, $r^2 = 0.942$, *SEE* = 0.104, $F = 162.49$ and $r^2_{pred} = 0.779$ for five components. CoMFA electrostatic contours revealed that increased negative charge at the *meta* position of the 4-phenyl ring was favorable for the activity. They found that electron withdrawing groups at the *meta* and *para* positions around the anilino ring were important for enhancing activity. Electron-withdrawing bulky *ortho* substituents on the 4-phenyl ring were conducive to GSK-3*α* inhibition. CoMSIA model showed the importance of hydrogen bond donor groups on these ligands for enhanced activity. The best CoMSIA model (S + E + D) had $n = 56$, $q^2 = 0.833$, $r^2 = 0.932$, *SEE* = 0.113, $F = 111.67$ and $r^2_{pred} = 0.803$ for six components. Comparatively, 3-N-methylanilino derivatives were less active than 3-anilino derivatives.

Docking studies revealed the binding poses of three subclasses of these ligands, namely anilino, N-methylanilino and indoline derivatives, within the active site of the *β* isoform, and helped to explain the difference in their inhibitory activity.

3.3. QSAR Studies of Some GSK-3α Inhibitory Pyrimidines

Jamloky *et al.* in this paper [22] studied a series of pyrimidines which was performed to gain structural insight into the binding mode of the molecules to the GSK-3*α*. The molecular modeling studies were performed using CS Chem.

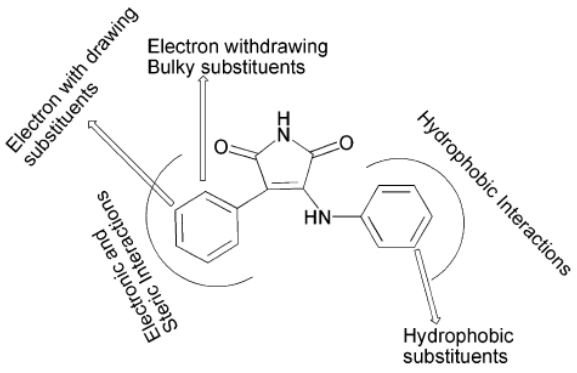

Fig. (8). Proposed model based on 2D-QSAR analyses showing the nature of interactions and substitution requirements for effective binding of 3-anilino-4-phenylmaleimides with the GSK-3*α* isoform.

Office 2001 molecular modeling software version 6.0. MOPAC module was used to minimized the energy and calculate of the descriptors. The thermodynamic and steric features of the pyrimidines were highly correlated with GSK-3*α* inhibitory activity. The positive coefficient of PMI-Y in the model suggested the presence of bulky substituents oriented towards Y-axis of the molecule will enhance the GSK-3*α* inhibitory activity. The observation supports the hypothesis that the presence of the bulky substituents like bromine with inherent hydrophobic character may involve in nonspecific interaction with the ATP binding site. The results of the study suggested that introduction of bulky groups at C-5 position of the hydrophobic interaction with the ATP binding site of the enzyme. This may be attributed to the strain exerted by the two adjacent phenyl rings on the planar pyrazolo (3,4-*b*) pyridine ring thereby partly disrupting the hydrogen bonding interaction between nitrogen in the pyrazolo group and the complementary group in the enzyme.

4. Studies of GSK-3β Inhibitors

4.1. Design, Synthesis and Structure-Activity Relationships of 1,3,4-oxadiazole Derivatives

Saitoh *et al.* [94] reported design, synthesis and structure–activity relationships of a novel series of oxadiazole derivatives as GSK-3*β* inhibitors. Among these inhibitors, compound 20x (see Figure) showed highly selective and potent GSK-3*β* inhibitory activity *in vitro* and its binding mode was determined by obtaining the X-ray co-crystal structure of 20x (see Fig. **9**) and GSK-3*β* (see Fig. **10**). The hydrogen bonding interaction of the benzimidazole core with the hinge region and the oxadiazole with Asp200 were observed. Additionally, interaction of 4-methoxyphenyl group with Arg141 was observed.

4.2. Linear/Nonlinear Regression Methods for Prediction of Glycogen Synthase Kinase-3β Inhibitory Activities

Freitas *et al.* [95] realized linear/nonlinear regression methods as multiple linear regression (MLR), artificial neural network (ANN), and support vector machines (SVM) with a series of glycogen synthase kinase-3*β* (GSK-3*β*) inhibitors using calculated Dragon descriptors. Few variables were selected from a pool of calculated Dragon descriptors through three different feature selection methods, namely genetic algorithm (GA), successive projections algorithm (SPA), and fuzzy rough set ant colony optimization (fuzzy rough set ACO). The fuzzy rough set ACO/SVM-based model gave the best estimation/prediction results, demonstrating the nonlinear nature of this analysis and suggesting fuzzy rough set ACO, first introduced in chemistry here, as an improved variable selection method in QSAR for the class of GSK-3*β* inhibitors. MLR yielded QSAR models only reasonably predictable, with r^2 ranging from 0.77 to 0.81 and r^2_{test} of 0.67 to 0.76, ANN and specially SVM were capable of estimating and predicting biological activities very accurately.

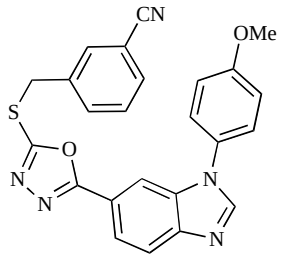

Fig. (9). Structure of 20x.

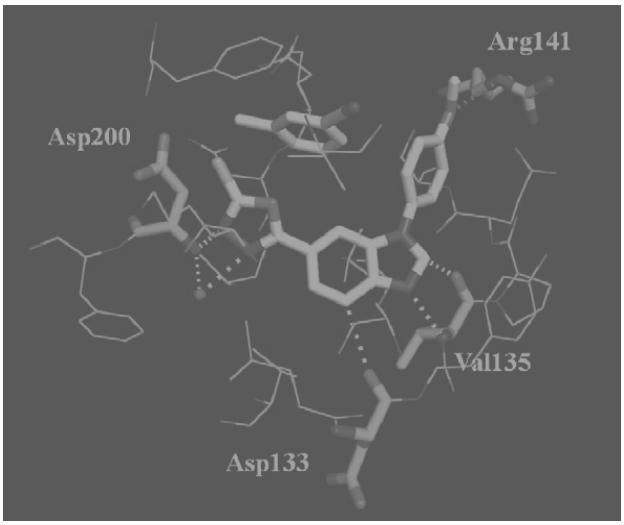

Fig. (10). X-ray co-crystal structure of 1 in complex with GSK-3*β*.

4.3. Molecular Modeling, Docking and 3D-QSAR Studies for Maleimides

Hwan-Kim *et al.* [96] in this article carried out molecular modeling and docking studies with three-dimensional quantitative structure relationships (3D-QSAR) to determinate the correct binding mode of glycogen synthase kinase 3*β* (GSK-3*β*) inhibitors. For the 3D-QSAR (CoMFA and CoMSIA), they used 51 substituted benzofuran-3-yl-(indol-3-yl)maleimides. Two binding modes of the inhibitors to the binding site of GSK-3*β* are investigated. The binding mode 1 yielded better 3D-QSAR correlations using both

CoMFA and CoMSIA methodologies. The three-component CoMFA model from the steric and electrostatic fields for the experimentally determined pIC_{50} values has the following statistics: $R^2(cv) = 0.386$ and $SE(cv) = 0.854$ for the cross-validation, and $R^2 = 0.811$ and $SE = 0.474$ for the fitted correlation. $F(3,47) = 67.034$, and probability of $R^2 = 0$ $(3,47)= 0.000$. The binding mode suggested by the results of this study was consistent with the preliminary results of X-ray crystal structures of inhibitor-bound GSK-3*β*. The 3D-QSAR models were used for the estimation of the inhibitory potency of two additional compounds.

4.4. Molecular Docking and Biological Testing of New Inhibitors of GSK-3β

Lavrovskii *et al*. [97] used in this paper a serie of new heteroaryl-substituted oxadiazole-5-carboxamide inhibitors of GSK-3*β*. Molecular docking was used for the rational selection of synthesized compounds for the subsequent biological testing. It was established that the inhibitory activity of the synthesized compounds strongly depends on the character of substituents in the phenyl ring and the nature of terminal heterocyclic fragments. The most active compounds inhibit GSK-3*β* at IC_{50} in the micro molar range and could be considered as potential drug candidates.

4.5. 3D-QSAR Modelling of Paullones

Osolodkin *et al*. [98] realized 3D-QSAR study allows one to suggest ways of modification of the molecule to increase its physiological activity. Comparative molecular field analysis (CoMFA) [7] and comparative molecular similarity indices analysis (CoMSIA) [8] are among the most widely used 3D-QSAR methods. The energy of van der Waals and electrostatic interactions of a probe atom (with the charge +1) with molecules of the training set (CoMFA) or the electrostatic, van der Waals, hydrophobic, and donor/acceptor similarity indices (CoMSIA) were used as descriptors. The equation for activity prediction was derived using the partial least squares (PLS) method. The ability of graphic representation of PLS model coefficients was the advantage of the methods and allowed the user to suggest substitutions affecting activity and/or selectivity of the molecules. They had built a new 3D-QSAR model for GSK-3*β* inhibition by paullones by means of CoMFA method. This model can be used as a guide for design of new paullone GSK-3*β* inhibitors.

4.6. Modeling of Binding Mode of Benzo[e]isoindole-1,3-diones

Yang *et al*. [99] synthesized benzo[*e*]isoindole-1,3-dione derivatives, and the effects on GSK-3*β* activity and zebrafish embryo growth were evaluated. A series of derivatives showed obvious inhibitory activity against GSK-3*β*. The most potent inhibitor, 7,8-dimethoxy-5-methylbenzo[*e*] isoindole-1,3-dione, showed nanomolar IC_{50} and obvious phenotype on zebrafish embryo growth associated with the inhibition of GSK-3*β* at low micro molar concentration. The interaction mode between this compound and GSK-3*β* was characterized by computational modeling. To rationalize the structure-activity relationships of these compounds, the binding modes of the most potent inhibitors 8a and 8b (see Fig. **11**) were modeled using docking simulations. Compounds 8a and 8b were docked into the ATP binding site of GSK-3*β*, and the binding modes of lowest energy were analyzed. Compounds 8a and 8b fit the ATP pocket of GSK-3*β* well. The maleimide motif of type II formed a pair of hydrogen bonds with the hinge region (Glu133 and Val135) of GSK-3*β*, similar to the binding mode of other known maleimides GSK-3*β* inhibitors. The two methoxy oxygen atoms formed another two hydrogen bonds with the positively charged Lys85. The methyl group of the methoxy at C-8 position docked to the small back cleft of GSK-3*β*. This binding mode explicitly explained the important role of the two methoxy groups at C-7 and C-8 positions. Other result was the 4-ethyl group of 8b docks to the minor hydrophobic pocket formed by Ile62 and Val70 in the front of the ATP binding site of GSK-3*β* (Fig. **12**), which contributed to its higher binding affinity compared to 8a. The docking results also provided a template to understand the structure-activity relationships of other compounds.

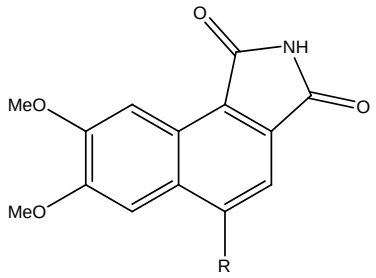

8a: R = Me
8b: R = Et

Fig. (11). Structure of **8a** and **8b**.

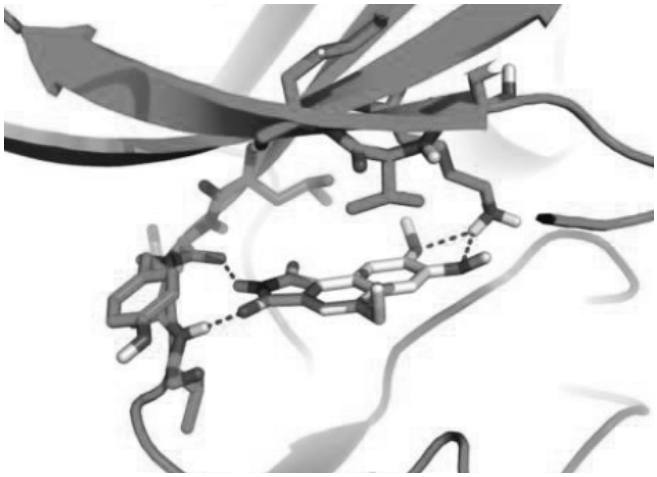

Fig. (12). Docked binding modes of compounds **8b** in the ATP binding site of GSK-3*β*.

CONCLUSIONS

Theoretical studies such as QSAR models have become a very useful tool in this context to substantially reduce time and resources consuming experiments. The functions of *β* and *γ*-secretase and its implication in Alzheimer's disease have triggered an active search for potent and selective *β* and

γ-secretase inhibitors. In this paper we can see that the development of theoretical and QSAR models to study γ-secretase inhibitors are usually not many achieved so far, and most of these works present docking studies. Watching this situation we need to develop QSAR models with γ-secretase inhibitors. In this sense, QSAR could play an important role in studying these γ-secretase inhibitors. QSARs can be used as predictive tools for the development of molecules. In this work we developed a new ANN RBF model using the ModesLab descriptors, based on a large database using about 10,000 different drugs obtained from the ChEMBL server.

CONFLICT OF INTEREST

None declared.

ACKNOWLEDGEMENTS

Prado-Prado F. thanks sponsorships for research position at the University of Santiago de Compostela from *Angeles Alvariño*, Xunta de Galicia. All authors acknowledge the Project 07CSA008203PR.

REFERENCES

[1] Golde, T. E., Dickson, D. and Hutton, M., Filling the gaps in the abeta cascade hypothesis of Alzheimer's disease. *Curr Alzheimer Res*, **2006**, 3, 421-30

[2] Hutton, M., Perez-Tur, J. and Hardy, J., Genetics of Alzheimer's disease. *Essays Biochem*, **1998**, 33, 117-31

[3] Younkin, S. G., The role of A beta 42 in Alzheimer's disease. *J Physiol Paris*, **1998**, 92, 289-92

[4] Sisodia, S. S., Alzheimer's disease: perspectives for the new millennium. *J Clin Invest*, **1999**, 104, 1169-70

[5] Rovelet-Lecrux, A., Hannequin, D., Raux, G., Le Meur, N., Laquerriere, A., Vital, A., Dumanchin, C., Feuillette, S., Brice, A., Vercelletto, M., Dubas, F., Frebourg, T. and Campion, D., APP locus duplication causes autosomal dominant early-onset Alzheimer disease with cerebral amyloid angiopathy. *Nat Genet*, **2006**, 38, 24-6

[6] Ohno, M., Sametsky, E. A., Younkin, L. H., Oakley, H., Younkin, S. G., Citron, M., Vassar, R. and Disterhoft, J. F., BACE1 deficiency rescues memory deficits and cholinergic dysfunction in a mouse model of Alzheimer's disease. *Neuron*, **2004**, 41, 27-33

[7] Ohno, M., Cole, S. L., Yasvoina, M., Zhao, J., Citron, M., Berry, R., Disterhoft, J. F. and Vassar, R., BACE1 gene deletion prevents neuron loss and memory deficits in 5XFAD APP/PS1 transgenic mice. *Neurobiol Dis*, **2007**, 26, 134-45

[8] Laird, F. M., Cai, H., Savonenko, A. V., Farah, M. H., He, K., Melnikova, T., Wen, H., Chiang, H. C., Xu, G., Koliatsos, V. E., Borchelt, D. R., Price, D. L., Lee, H. K. and Wong, P. C., BACE1, a major determinant of selective vulnerability of the brain to amyloid-beta amyloidogenesis, is essential for cognitive, emotional, and synaptic functions. *J Neurosci*, **2005**, 25, 11693-709

[9] Selkoe, D. J., Alzheimer's disease: genes, proteins, and therapy. *Physiol Rev*, **2001**, 81, 741-66

[10] Vassar, R., BACE1: the beta-secretase enzyme in Alzheimer's disease. *J Mol Neurosci*, **2004**, 23, 105-14

[11] Hussain, I., Powell, D., Howlett, D. R., Tew, D. G., Meek, T. D., Chapman, C., Gloger, I. S., Murphy, K. E., Southan, C. D., Ryan, D. M., Smith, T. S., Simmons, D. L., Walsh, F. S., Dingwall, C. and Christie, G., Identification of a novel aspartic protease (Asp 2) as beta-secretase. *Mol Cell Neurosci*, **1999**, 14, 419-27

[12] Sinha, S., Anderson, J. P., Barbour, R., Basi, G. S., Caccavello, R., Davis, D., Doan, M., Dovey, H. F., Frigon, N., Hong, J., Jacobson-Croak, K., Jewett, N., Keim, P., Knops, J., Lieberburg, I., Power, M., Tan, H., Tatsuno, G., Tung, J., Schenk, D., Seubert, P., Suomensaari, S. M., Wang, S., Walker, D., Zhao, J., McConlogue, L. and John, V., Purification and cloning of amyloid precursor protein beta-secretase from human brain. *Nature*, **1999**, 402, 537-40

[13] Vassar, R., Bennett, B. D., Babu-Khan, S., Kahn, S., Mendiaz, E. A., Denis, P., Teplow, D. B., Ross, S., Amarante, P., Loeloff, R., Luo, Y., Fisher, S., Fuller, J., Edenson, S., Lile, J., Jarosinski, M. A., Biere, A. L., Curran, E., Burgess, T., Louis, J. C., Collins, F., Treanor, J., Rogers, G. and Citron, M., Beta-secretase cleavage of Alzheimer's amyloid precursor protein by the transmembrane aspartic protease BACE. *Science*, **1999**, 286, 735-41

[14] Yan, R., Bienkowski, M. J., Shuck, M. E., Miao, H., Tory, M. C., Pauley, A. M., Brashier, J. R., Stratman, N. C., Mathews, W. R., Buhl, A. E., Carter, D. B., Tomasselli, A. G., Parodi, L. A., Heinrikson, R. L. and Gurney, M. E., Membrane-anchored aspartyl protease with Alzheimer's disease beta-secretase activity. *Nature*, **1999**, 402, 533-7

[15] Goate, A., Chartier-Harlin, M. C., Mullan, M., Brown, J., Crawford, F., Fidani, L., Giuffra, L., Haynes, A., Irving, N., James, L. and *et al*., Segregation of a missense mutation in the amyloid precursor protein gene with familial Alzheimer's disease. *Nature*, **1991**, 349, 704-6

[16] Schellenberg, G. D., Bird, T. D., Wijsman, E. M., Orr, H. T., Anderson, L., Nemens, E., White, J. A., Bonnycastle, L., Weber, J. L., Alonso, M. E. and *et al*., Genetic linkage evidence for a familial Alzheimer's disease locus on chromosome 14. *Science*, **1992**, 258, 668-71

[17] Haass, C., Schlossmacher, M. G., Hung, A. Y., Vigo-Pelfrey, C., Mellon, A., Ostaszewski, B. L., Lieberburg, I., Koo, E. H., Schenk, D., Teplow, D. B. and *et al*., Amyloid beta-peptide is produced by cultured cells during normal metabolism. *Nature*, **1992**, 359, 322-5

[18] Seubert, P., Oltersdorf, T., Lee, M. G., Barbour, R., Blomquist, C., Davis, D. L., Bryant, K., Fritz, L. C., Galasko, D., Thal, L. J. and *et al*., Secretion of beta-amyloid precursor protein cleaved at the amino terminus of the beta-amyloid peptide. *Nature*, **1993**, 361, 260-3

[19] Zhao, J., Paganini, L., Mucke, L., Gordon, M., Refolo, L., Carman, M., Sinha, S., Oltersdorf, T., Lieberburg, I. and McConlogue, L., Beta-secretase processing of the beta-amyloid precursor protein in transgenic mice is efficient in neurons but inefficient in astrocytes. *J Biol Chem*, **1996**, 271, 31407-11

[20] Citron, M., Teplow, D. B. and Selkoe, D. J., Generation of amyloid beta protein from its precursor is sequence specific. *Neuron*, **1995**, 14, 661-70

[21] Phiel, C. J., Wilson, C. A., Lee, V. M.-Y. and Klein, P. S., GSK-3α regulates production of Alzheimer's disease amyloid-β peptides. *Nature*, **2003**, 423, 435-439

[22] Jamloki, A., Karthikeyan, C. and Sharma, S. K., QSAR Studies on Some GSK-3α Inhibitory 6-aryl-pyrazolo-(3,4-b)pyrimidines. *Asian Journal of Biochemistry*, **2006**, 1, 236-243

[23] Ali, A., Hoeflich, K. P. and Woodgett, J. R., Glycogen Synthase Kinase-3: Properties, Functions, and Regulation. *Chem Rev*, **2001**, 101, 2527-2540

[24] Martinez, A., Castro, A., Dorronsoro, I. and Alonso, M., Glycogen synthase kinase 3 (GSK-3) inhibitors as new promising drugs for diabetes, neurodegeneration, cancer, and inflammation. *Med Res Rev*, **2002**, 22, 373-84

[25] Martinez, A., Alonso, M., Castro, A., Perez, C. and Moreno, F. J., First Non-ATP Competitive Glycogen Synthase Kinase 3B (GSK-3B) Inhibitors: Thiadazolidinones (TDZD) as Potential Drugs for the Treatment of Alzheimer´s Disease. *J Med Chem*, **2002**, 45, 1292-1299

[26] Hagit, E.-F., Glycogen synthase kinase 3: an emerging therapeutic target. *Trends in Molecular Medicine*, **2002**, 8, 126-132

[27] Lee, V. M., Goedert, M. and Trojanowski, J. Q., Neurodegenerative tauopathies. *Ann Rev Neurosci*, **2001**, 24, 1121-1159

[28] Flaherty, D. B., Sorrea, P. J., Tomasienicz, G. H. and Wood, G. J., Phosphorilation of human tau protein by microtubule-associated kinases: GSK3beta and cdk5 are key participants. *J Neuro Sci Res*, **2000**, 62, 463-472

[29] Bhat, R. V., Budd Haeberlein, S. L. and Avila, J. J., Glycogen synthase kinase 3: a drug target for CNS therapies. *J Neurochem*, **2004**, 89, 1313-1317

[30] Sivaprakasam, P., Xiea, A. and Doerksen, R. J., Probing the physicochemical and structural requirements for glycogen synthase kinase-3a inhibition: 2D-QSAR for 3-anilino-4-phenylmaleimides. *Bioorganic & Medicinal Chemistry Letters*, **2006**, 14, 8210-8218

[31] Ishiguro, K., Takamatsu, M., Tomizawa, K., Omori, A., Takahashi, M., Arioka, M., Uchida, T. and Imahori, K., Tau protein kinase I

converts normal tau protein into A68-like component of paired helical filaments. *J. Biol. Chem.*, **1992**, 267, 10897-10901

[32] Pei, J. J., Tanaka, T., Tung, Y. C., Braak, E., Iqbal, K. and Grundke-Iqbal, I., Distribution, Levels, and Activity of Glycogen Synthase Kinase-3 in the Alzheimer Disease Brain. *J. Neuropathol. Exp. Neurol.*, **1997**, 56, 70-78

[33] Pei, J. J., Braak, H., Grundke-Iqbal, I., Iqbal, K., Winblad, B. and Cowburn, R. F., Distribution of active glycogen synthase kinase 3beta (GSK-3beta) in brains staged for Alzheimer disease neurofibrillary changes. *J. Neuropathol. Exp. Neurol.*, **1999**, 58, 1010-1019

[34] Baum, L., Hansen, L., Masliah, E. and Saitoh, T., Glycogen synthase kinase 3 alteration in Alzheimer disease is related to neurofibrillary tangle formation. *Mol. Chem. Neuropathol.*, **1996**, 29, 253-261

[35] Lucas, J. J., Hernandez, F., Gomez-Ramos, P., Moran, M. A., Hen, R. and Avila, J., Decreased nuclear -catenin, tau hyperphosphorylation and neurodegeneration in GSK-3 conditional transgenic mice. *EMBO J.*, **2001**, 20, 27-39

[36] Hernandez, F., Borrell, J., Guaza, C., Avila, J. and Lucas, J. J., Spatial learning deficit in transgenic mice that conditionally over-express GSK-3beta in the brain but do not form tau filaments. *J. Neurochem.*, **2002**, 83, 1529-1533

[37] Santana, L., Uriarte, E., González-Díaz, H., Zagotto, G., Soto-Otero, R. and Mendez-Alvarez, E., A QSAR model for in silico screening of MAO-A inhibitors. Prediction, synthesis, and biological assay of novel coumarins. *J Med Chem*, **2006**, 49, 1149-56

[38] Marrero-Ponce, Y., Linear indices of the "molecular pseudograph's atom adjacency matrix": definition, significance-interpretation, and application to QSAR analysis of flavone derivatives as HIV-1 integrase inhibitors. *J Chem Inf Comput Sci*, **2004**, 44, 2010-26

[39] Vilar, S., Santana, L. and Uriarte, E., Probabilistic neural network model for the in silico evaluation of anti-HIV activity and mechanism of action. *J Med Chem* **2006**, 49, 1118-1124

[40] Marrero-Ponce, Y., Khan, M. T., Casanola Martin, G. M., Ather, A., Sultankhodzhaev, M. N., Torrens, F. and Rotondo, R., Prediction of tyrosinase inhibition activity using atom-based bilinear indices. *ChemMedChem*, **2007**, 2, 449-78

[41] Casanola-Martin, G. M., Marrero-Ponce, Y., Khan, M. T., Ather, A., Sultan, S., Torrens, F. and Rotondo, R., TOMOCOMD-CARDD descriptors-based virtual screening of tyrosinase inhibitors: evaluation of different classification model combinations using bond-based linear indices. *Bioorg Med Chem*, **2007**, 15, 1483-503

[42] Casanola-Martin, G. M., Marrero-Ponce, Y., Khan, M. T., Ather, A., Khan, K. M., Torrens, F. and Rotondo, R., Dragon method for finding novel tyrosinase inhibitors: Biosilico identification and experimental *in vitro* assays. *Eur J Med Chem*, **2007**, 42, 1370-81

[43] Nunez, M. B., Maguna, F. P., Okulik, N. B. and Castro, E. A., QSAR modeling of the MAO inhibitory activity of xanthones derivatives. *Bioorg Med Chem Lett*, **2004**, 14, 5611-5617

[44] Todeschini, R. and Consonni, V., Handbook of Molecular Descriptors. *Wiley VCH*, **2000**,

[45] González-Díaz, H., González-Díaz, Y., Santana, L., Ubeira, F. M. and Uriarte, E., Proteomics, networks and connectivity indices. *Proteomics*, **2008**, 8, 750-778

[46] Zhao, C. J. and Dai, Q. Y., [Recent advances in study of antinociceptive conotoxins]. *Yao Xue Xue Bao*, **2009**, 44, 561-5

[47] Jacob, R. B. and McDougal, O. M., The M-superfamily of conotoxins: a review. *Cellular and Molecular Life Sciences*, **2010**, 67, 17-27

[48] Giuliani, A., Di Paola, L. and Setola, R., Proteins as Networks: A Mesoscopic Approach Using Haemoglobin Molecule as Case Study. *Curr Proteomics*, **2009**, 6, 235-245

[49] Vilar, S., Gonzalez-Diaz, H., Santana, L. and Uriarte, E., A network-QSAR model for prediction of genetic-component biomarkers in human colorectal cancer. *Journal of Theoretical Biology*, **2009**, 261, 449-58

[50] Concu, R., Dea-Ayuela, M. A., Perez-Montoto, L. G., Prado-Prado, F. J., Uriarte, E., Bolas-Fernandez, F., Podda, G., Pazos, A., Munteanu, C. R., Ubeira, F. M. and Gonzalez-Diaz, H., 3D entropy and moments prediction of enzyme classes and experimental-theoretic study of peptide fingerprints in Leishmania parasites. *Biochimica et Biophysica Acta*, **2009**, 1794, 1784-94

[51] Torrens, F. and Castellano, G., Topological Charge-Transfer Indices: From Small Molecules to Proteins. *Curr Proteomics*, **2009**, 204-213

[52] Vázquez, J. M., Aguiar, V., Seoane, J. A., Freire, A., Serantes, J. A., Dorado, J., Pazos, A. and Munteanu, C. R., Star Graphs of Protein Sequences and Proteome Mass Spectra in Cancer Prediction. *Curr Proteomics*, **2009**, 6, 275-288

[53] Gonzalez-Diaz, H., Quantitative studies on Structure-Activity and Structure-Property Relationships (QSAR/QSPR). *Curr Top Med Chem*, **2008**, 8, 1554

[54] Ivanciuc, O., Weka machine learning for predicting the phospholipidosis inducing potential. *Curr Top Med Chem*, **2008**, 8, 1691-709

[55] Gonzalez-Díaz, H., Prado-Prado, F. and Ubeira, F. M., Predicting antimicrobial drugs and targets with the MARCH-INSIDE approach. *Curr Top Med Chem*, **2008**, 8, 1676-90

[56] Duardo-Sanchez, A., Patlewicz, G. and Lopez-Diaz, A., Current topics on software use in medicinal chemistry: intellectual property, taxes, and regulatory issues. *Curr Top Med Chem*, **2008**, 8, 1666-75

[57] Wang, J. F., Wei, D. Q. and Chou, K. C., Drug candidates from traditional chinese medicines. *Curr Top Med Chem*, **2008**, 8, 1656-65

[58] Helguera, A. M., Combes, R. D., Gonzalez, M. P. and Cordeiro, M. N., Applications of 2D descriptors in drug design: a DRAGON tale. *Curr Top Med Chem*, **2008**, 8, 1628-55

[59] Gonzalez, M. P., Teran, C., Saiz-Urra, L. and Teijeira, M., Variable selection methods in QSAR: an overview. *Curr Top Med Chem*, **2008**, 8, 1606-27

[60] Caballero, J. and Fernandez, M., Artificial neural networks from MATLAB in medicinal chemistry. Bayesian-regularized genetic neural networks (BRGNN): application to the prediction of the antagonistic activity against human platelet thrombin receptor (PAR-1). *Curr Top Med Chem*, **2008**, 8, 1580-605

[61] Wang, J. F., Wei, D. Q. and Chou, K. C., Pharmacogenomics and personalized use of drugs. *Curr Top Med Chem*, **2008**, 8, 1573-9

[62] Vilar, S., Cozza, G. and Moro, S., Medicinal chemistry and the molecular operating environment (MOE): application of QSAR and molecular docking to drug discovery. *Curr Top Med Chem*, **2008**, 8, 1555-72

[63] Prado-Prado, F. J., Garcia-Mera, X. and Gonzalez-Diaz, H., Multi-target spectral moment QSAR versus ANN for antiparasitic drugs against different parasite species. *Bioorg Med Chem*, **2010**, 18, 2225-31

[64] Gonzalez-Diaz, H., Network topological indices, drug metabolism, and distribution. *Curr Drug Metab*, 11, 283-4

[65] Khan, M. T., Predictions of the ADMET properties of candidate drug molecules utilizing different QSAR/QSPR modelling approaches. *Curr Drug Metab*, 11, 285-95

[66] Mrabet, Y. and Semmar, N., Mathematical methods to analysis of topology, functional variability and evolution of metabolic systems based on different decomposition concepts. *Curr Drug Metab*, 11, 315-41

[67] Martinez-Romero, M., Vazquez-Naya, J. M., Rabunal, J. R., Pita-Fernandez, S., Macenlle, R., Castro-Alvarino, J., Lopez-Roses, L., Ulla, J. L., Martinez-Calvo, A. V., Vazquez, S., Pereira, J., Porto-Pazos, A. B., Dorado, J., Pazos, A. and Munteanu, C. R., Artificial intelligence techniques for colorectal cancer drug metabolism: ontology and complex network. *Curr Drug Metab*, 11, 347-68

[68] Zhong, W. Z., Zhan, J., Kang, P. and Yamazaki, S., Gender specific drug metabolism of PF-02341066 in rats--role of sulfoconjugation. *Curr Drug Metab*, 11, 296-306

[69] Wang, J. F. and Chou, K. C., Molecular modeling of cytochrome P450 and drug metabolism. *Curr Drug Metab*, 11, 342-6

[70] Gonzalez-Diaz, H., Duardo-Sanchez, A., Ubeira, F. M., Prado-Prado, F., Perez-Montoto, L. G., Concu, R., Podda, G. and Shen, B., Review of MARCH-INSIDE & complex networks prediction of drugs: ADMET, anti-parasite activity, metabolizing enzymes and cardiotoxicity proteome biomarkers. *Curr Drug Metab*, 11, 379-406

[71] Garcia, I., Diop, Y. F. and Gomez, G., QSAR & complex network study of the HMGR inhibitors structural diversity. *Curr Drug Metab*, 11, 307-14

[72] Chou, K. C., Graphic rule for drug metabolism systems. *Curr Drug Metab*, 11, 369-78

[73] Concu, R., Podda, G., Ubeira, F. M. and Gonzalez-Diaz, H., Review of QSAR Models for Enzyme Classes of Drug Targets: Theoretical Background and Applications in Parasites, Hosts, and other Organisms. *Current Pharmaceutical Design*, **2010**, 16, 2710-23

[74] Estrada, E., Molina, E., Nodarse, D. and Uriarte, E., Structural Contributions of Substrates to their Binding to P-Glycoprotein. A TOPS-MODE Approach. *Current Pharmaceutical Design*, **2010**, 16, 2676-709

[75] Garcia, I., Fall, Y. and Gomez, G., QSAR, Docking, and CoMFA Studies of GSK3 Inhibitors. *Current Pharmaceutical Design*, **2010**, 16, 2666-75

[76] González-Díaz, H., QSAR and Complex Networks in Pharmaceutical Design, Microbiology, Parasitology, Toxicology, Cancer, and Neurosciences. *Current Pharmaceutical Design*, **2010**, 16, 2598-600

[77] Gonzalez-Diaz, H., Romaris, F., Duardo-Sanchez, A., Perez-Mototo, L. G., Prado-Prado, F., Patlewicz, G. and Ubeira, F. M., Predicting drugs and proteins in parasite infections with topological indices of complex networks: theoretical backgrounds, aplications, and legal issues. *Current Pharmaceutical Design*, **2010**, 16, 2737-64

[78] Marrero-Ponce, Y., Casanola-Martin, G. M., Khan, M. T., Torrens, F., Rescigno, A. and Abad, C., Ligand-Based Computer-Aided Discovery of Tyrosinase Inhibitors. Applications of the TOMOCOMD-CARDD Method to the Elucidation of New Compounds. *Current Pharmaceutical Design*, **2010**, 16, 2601-24

[79] Munteanu, C. R., Fernandez-Blanco, E., Seoane, J. A., Izquierdo-Novo, P., Rodriguez-Fernandez, J. A., Prieto-Gonzalez, J. M., Rabunal, J. R. and Pazos, A., Drug Discovery and Design for Complex Diseases through QSAR Computational Methods. *Current Pharmaceutical Design*, **2010**, 16, 2640-55

[80] Roy, K. and Ghosh, G., Exploring QSARs with Extended Topochemical Atom (ETA) Indices for Modeling Chemical and Drug Toxicity. *Current Pharmaceutical Design*, **2010**, 16, 2625-39

[81] Speck-Planche, A., Scotti, M. T. and de Paulo-Emerenciano, V., Current pharmaceutical design of antituberculosis drugs: future perspectives. *Current Pharmaceutical Design*, **2010**, 16, 2656-65

[82] Vazquez-Naya, J. M., Martinez-Romero, M., Porto-Pazos, A. B., Novoa, F., Valladares-Ayerbes, M., Pereira, J., Munteanu, C. R. and Dorado, J., Ontologies of drug discovery and design for neurology, cardiology and oncology. *Current Pharmaceutical Design*, **2010**, 16, 2724-36

[83] Garcia, I., Diop, Y. F. and Gomez, G., QSAR & complex network study of the HMGR inhibitors structural diversity. *Curr Drug Metab*, **2010**, 11, 307-14

[84] Choi, S. J., Cho, J. H., Im, I., Lee, S. D., Jang, J. Y., Oh, Y. M., Jung, Y. K., Jeon, E. S. and Kim, Y. C., Design and synthesis of 1,4-dihydropyridine derivatives as BACE-1 inhibitors. *Eur J Med Chem*, **2010**, 45, 2578-90

[85] Yi Mok, N., Chadwick, J., Kellett, K. A., Hooper, N. M., Johnson, A. P. and Fishwick, C. W., Discovery of novel non-peptide inhibitors of BACE-1 using virtual high-throughput screening. *Bioorg Med Chem Lett*, **2009**, 19, 6770-4

[86] Sato, T., Ananda, K., Cheng, C. I., Suh, E. J., Narayanan, S. and Wolfe, M. S., Distinct pharmacological effects of inhibitors of signal peptide peptidase and gamma-secretase. *J Biol Chem*, **2008**, 283, 33287-95

[87] Sammi, T., Silakari, O. and Ravikumar, M., Three-dimensional quantitative structure-activity relationship (3D-QSAR) studies of various benzodiazepine analogues of gamma-secretase inhibitors. *J Mol Model*, **2009**, 15, 343-8

[88] Al-Nadaf, A., Abu Sheikha, G. and Taha, M. O., Elaborate ligand-based pharmacophore exploration and QSAR analysis guide the synthesis of novel pyridinium-based potent beta-secretase inhibitory leads. *Bioorg Med Chem*, **2010**, 18, 3088-115

[89] Pandey, A., Mungalpara, J. and Mohan, C. G., Comparative molecular field analysis and comparative molecular similarity indices analysis of hydroxyethylamine derivatives as selective human BACE-1 inhibitor. *Mol Divers*, **2010**, 14, 39-49

[90] Polgar, T. and Keseru, G. M., Virtual screening for beta-secretase (BACE1) inhibitors reveals the importance of protonation states at Asp32 and Asp228. *J Med Chem*, **2005**, 48, 3749-55

[91] Hetenyi, C., Paragi, G., Maran, U., Timar, Z., Karelson, M. and Penke, B., Combination of a modified scoring function with two-dimensional descriptors for calculation of binding affinities of bulky, flexible ligands to proteins. *J Am Chem Soc*, **2006**, 128, 1233-9

[92] Moitessier, N., Therrien, E. and Hanessian, S., A method for induced-fit docking, scoring, and ranking of flexible ligands. Application to peptidic and pseudopeptidic beta-secretase (BACE 1) inhibitors. *J Med Chem*, **2006**, 49, 5885-94

[93] Sivaprakasam, P., Daga, P. R., Xie, A. and Doerksen, R. J., Glycogen synthase kinase-3 inhibition by 3-anilino-4-phenylmaleimides: insights from 3D-QSAR and docking. *J Comput Aided Mol Des*, **2009**, 23, 113-127

[94] Saitoh, M., Kunitomo, J., Kimura, E., Hayase, Y., Kobayashi, H., Uchiyama, N., Kawamoto, T., Tanaka, T., Mol, C. D., Dougan, D. R., Textor, G. S., Snell, G. P. and Itoh, F., Design, synthesis and structure–activity relationships of 1,3,4-oxadiazole derivatives as novel inhibitors of glycogen synthase kinase-3beta. *Bioorganic & Medicinal Chemistry*, **2009**, 17, 2017-2029

[95] Freitas, M. P., Goodarzi, M. and Jensen, R., Feature Selection and Linear/Nonlinear Regression Methods for the Accurate Prediction of Glycogen Synthase Kinase-3β Inhibitory Activities *Journal of Chemical Information and Modeling* **2009**, 49, 824-832

[96] Kim, K. H., Gaisina, I., Gallier, F., Holzle, D., Blond, S. Y., Mesecar, A. and Kozikowski, A. P., Use of molecular modeling, docking, and 3D-QSAR studies for the determination of the binding mode of benzofuran-3-yl-(indol-3-yl)maleimides as GSK-3β inhibitors. *J Mol Model*, **2009**, 15, 1463-1479

[97] Ryzhova, E. A., Koryakova, A. G., Bulanova, E. A., Mikitas, O. V., Karapetyan, R. N., Lavrovskii, Y. V. and Ivashchenko, A. V., Syntheis, Molecular Docking, and Biological Testing of New Selective Inhibitors of Glycogen Synthase Kinase 3beta. *Pharmaceutical Chemistry Journal*, **2009**, 43, 148-153

[98] Osolodkin, D. I., Shulga, D. A., Tsareva, D. A., Oliferenko, A. A., Palyulin, V. A. and Zefirov, N. S., The Choice of Atomic Charges Calculation Scheme in 3D-QSAR Modelling of GSK-3β Inhibition by Paullones. *Biochemistry, Biophysics and Molecular Biology*, **2010**, 434, 274-278

[99] Zou, H., Zhou, L., Li, Y., Cui, Y., Zhong, H., Pan, Z., Yang, Z. and Quan, J., Benzo[e]isoindole-1,3-diones as Potential Inhibitors of Glycogen Synthase Kinase-3 (GSK-3). Synthesis, Kinase Inhibitory Activity, Zebrafish Phenotype, and Modeling of Binding Mode. *J. Med. Chem.*, **2010**, 53, 994-1003.

Received: November 23, 2010 Revised: February 02, 2011 Accepted: March 02, 2011